Suboptimal Acclimation of Photosynthesis to Light in Wheat Canopies[1][CC-BY]

Alexandra J. Townsend,[a,b,2,3] Renata Retkute,[a,c] Kannan Chinnathambi,[a] Jamie W. P. Randall,[a] John Foulkes,[a] Elizabete Carmo-Silva,[d] and Erik H. Murchie[a]

[a]Division of Plant and Crop Science, School of Biosciences, University of Nottingham, Sutton Bonington Campus, Loughborough LE12 5RD, United Kingdom
[b]Crops for the Future, Jalan Broga, 43500 Semenyih Selangor Darul Ehsan, Malaysia
[c]School of Life Sciences, Gibbet Hill Campus, University of Warwick, Coventry CV4 7AL, United Kingdom
[d]Lancaster Environment Centre, Lancaster University, Lancaster LA1 4YQ, United Kingdom

ORCID IDs: 0000-0002-1621-6821 (A.J.T.); 0000-0002-3877-6440 (R.R.); 0000-0001-6059-9359 (E.C.-S.); 0000-0002-7465-845X (E.H.M.).

Photosynthetic acclimation (photoacclimation) is the process whereby leaves alter their morphology and/or biochemistry to optimize photosynthetic efficiency and productivity according to long-term changes in the light environment. The three-dimensional architecture of plant canopies imposes complex light dynamics, but the drivers for photoacclimation in such fluctuating environments are poorly understood. A technique for high-resolution three-dimensional reconstruction was combined with ray tracing to simulate a daily time course of radiation profiles for architecturally contrasting field-grown wheat (*Triticum aestivum*) canopies. An empirical model of photoacclimation was adapted to predict the optimal distribution of photosynthesis according to the fluctuating light patterns throughout the canopies. While the photoacclimation model output showed good correlation with field-measured gas-exchange data at the top of the canopy, it predicted a lower optimal light-saturated rate of photosynthesis at the base. Leaf Rubisco and protein contents were consistent with the measured optimal light-saturated rate of photosynthesis. We conclude that, although the photosynthetic capacity of leaves is high enough to exploit brief periods of high light within the canopy (particularly toward the base), the frequency and duration of such sunflecks are too small to make acclimation a viable strategy in terms of carbon gain. This suboptimal acclimation renders a large portion of residual photosynthetic capacity unused and reduces photosynthetic nitrogen use efficiency at the canopy level, with further implications for photosynthetic productivity. It is argued that (1) this represents an untapped source of photosynthetic potential and (2) canopy nitrogen could be lowered with no detriment to carbon gain or grain protein content.

The arrangement of plant material in time and space can result in a heterogenous and temporally unpredictable light environment. This is especially true within crop canopies, where leaf and stem architectural features can lead to complex patterns of light according to solar movement, weather, and wind. This is likely to influence productivity, because photosynthesis is highly responsive to changes in light intensity over short time scales (seconds to minutes). Leaf photosynthesis does not respond instantaneously to a sudden change in light level: the delay before steady state is reached is closely linked to the photosynthetic induction state, which is a physiological condition dependent on the leaf's recent light history (Sassenrath-Cole and Pearcy, 1994; Stegemann et al., 1999). The induction state is defined by factors including the activation state of photosynthetic enzymes (Yamori et al., 2012; Carmo-Silva and Salvucci, 2013), stomatal opening (Lawson and Blatt, 2014), and photoprotection (Hubbart et al., 2012). Together, these determine the speed with which a leaf can respond to an increase, or decrease, in light intensity. It is thought that these processes are not always coordinated for optimal productivity in fluctuating light, as shown by the slow recovery of quantum efficiency for CO_2 assimilation in low light (Zhu et al., 2004), high nonphotochemical quenching during induction (Hubbart et al., 2012; Kromdijk et al., 2016), and slow stomatal opening and closure (Lawson and Blatt,

[1] This project was funded by the Biotechnology and Biological Sciences Research Council BBSRC [grant BB/JOO3999/1]. A.J.T. received funding from Crops for the Future under project BioP1-006 and the School of Biosciences, University of Nottingham. The wheat BC_3 lines were developed as part of the BBSRC [grant BB/D008972].

[2] Current address: School of Biological and Chemical Sciences, Queen Mary University of London, London E1 4NS, UK.
[3] Address correspondence to alexandra.townsend@nottingham.ac.uk.

The author responsible for distribution of materials integral to the findings presented in this article in accordance with the policy described in the Instructions for Authors (www.plantphysiol.org) is: Alexandra J. Townsend (alexandra.townsend@nottingham.ac.uk).

A.J.T., R.R., and E.H.M. conceived the original screening and research plans; E.H.M. and J.F. supervised the experiments; A.J.T. performed most of the experiments with assistance from K.C. and J.W.P.R.; E.C.-S. carried out Rubisco assays and analysis; A.J.T. and R.R. designed the modeling experiments and analyzed the data; A.J.T. wrote the article with contributions of all the authors; E.H.M. supervised and made a substantial contribution to the writing.

www.plantphysiol.org/cgi/doi/10.1104/pp.17.01213

2014). It is predicted that such slow responses of photosynthesis to the environment can have a substantial impact on wheat (*Triticum aestivum*) yield (Taylor and Long, 2017).

The role of light-dependent changes in crop canopies has not had sufficient attention. The acclimation of photosynthesis to changes in light intensity and quality (here termed photoacclimation in order to distinguish it from the acclimation to other environmental factors) is the process by which plants alter their structure and composition over long time periods (days and weeks) in response to the environment they experience. Photoacclimation can be broadly split into two types: photoacclimation that is determined during leaf development, including cell size and number plus leaf shape (Weston et al., 2000; Murchie et al., 2005), and photoacclimation that can occur within mature tissues (Anderson et al., 1995; Walters, 2005; Retkute et al., 2015). While the former is largely irreversible, the latter, here termed dynamic photoacclimation, can be reversible. Differences include changes in light-harvesting capacity (shown by the chlorophyll *a*:*b* ratio), chlorophyll per unit of N, electron transport capacity per unit of chlorophyll, and rate of electron transport capacity relative to Rubisco activity (Björkman, 1981; Evans, 1989; Evans and Poorter, 2001). This involves changes in the relative amounts of a number of primary components and processes, including light-harvesting pigment-protein complexes (LHC), Calvin cycle enzymes, and electron transport components such as the cytochrome *b*/*f* complex. It is normally considered that photoacclimation represents an economy of form and function, permitting higher capacity for carbon assimilation in high light while improving the quantum efficiency in low light (Björkman, 1981; Anderson and Osmund, 1987; Anderson et al., 1995; Murchie and Horton, 1997). This gives rise to the further concept that the plant must measure and predict changes in its environment to elicit the most efficient response. It is known that photoacclimation responses to fluctuating light can be complex (Vialet-Chabrand et al., 2017) and that the disruption of photoacclimation using mutants of Arabidopsis (*Arabidopsis thaliana*) results in a loss of fitness (Athanasiou et al., 2010).

Is photoacclimation optimized for crop canopies? It is assumed to improve productivity because, following long-term shifts in light intensity, it permits a higher rate of photosynthesis at high light and a higher quantum efficiency at low light. Over time, this will directly influence the ability of the canopy to convert intercepted radiation to biomass and grain yield and reduce the amount of absorbed solar energy in potentially wasteful processes such as nonphotochemical quenching (Zhu et al., 2010; Murchie and Reynolds, 2012; Kromdijk et al., 2016). However, this has never been tested empirically in crop canopies, which often possess complex light dynamics that are dependent on architecture (Burgess et al., 2015). Hence, we do not know which features of photoacclimation would make appropriate traits for crop improvement.

To solve this problem, we need to first understand the features of natural light that trigger photoacclimation (e.g. integrated light levels, the duration of high-low light periods, or the frequency of high-low light periods). Early work suggested that integrated photosynthetic photon flux density (PPFD) could be an important driver (Chabot et al., 1979; Watling et al., 1997); however, later work, using well-characterized artificial fluctuations, highlighted the importance of the duration of high and low light periods (Yin and Johnson, 2000; Retkute et al., 2015). Therefore, it follows that the precise characteristics of the light environment are important when determining if photoacclimation is operating in a manner that maintains fitness and productivity. Past theoretical work has tended to focus upon canopies with randomly distributed leaves in space (Werner et al., 2001; Zhu et al., 2004), with a few recent models using more complex and realistic architectural features (Song et al., 2013; Burgess et al., 2015). This necessitates the study of photoacclimation in the context of light dynamics within accurately reconstructed 3D plant canopies, because even moderate changes in architecture can have a large impact on light characteristics (Burgess et al., 2015). Photoacclimation to high light requires an energy source and resources (carbon, N, and others) in order to enhance, for example, Rubisco per unit of leaf area. It can be argued that a high-light-saturated photosynthetic capacity (P_{max}) is advantageous under low light because it enables the exploitation of high-light periods (sunflecks). However, maintenance of a thick high-light-acclimated leaf with a high P_{max} (and high chlorophyll) may impose a respiratory burden and influence the efficiency of photosynthesis under low light. The advantage of maintaining a high P_{max} then becomes dependent on the frequency and duration of high sunflecks in the canopy and how fast photosynthetic induction can occur in response to each fleck. Although this question has been addressed to an extent in the ecological literature (Hikosaka, 2016), it is still not known whether there is an advantage to maintaining a higher P_{max} lower in the crop canopy in order to exploit sunflecks (Pearcy, 1990) or whether architecture influences the potential gain. Again, it depends on knowing the precise 3D pattern or light over time and predicting its likely effect on photoacclimation.

A last consideration concerns how photoacclimation is influenced by phenology and physiology within the canopy. In a cereal such as wheat, development occurs initially in high light, followed by progressive shading by younger leaves. Hence, it might be expected that photoacclimation would track this change in light accurately. However, the photosynthetic system represents a significant sink for leaf N and other soil-derived mineral elements, and this sink will increase in size as the photosynthetic capacity of the leaf rises. It has been suggested that lower leaves in the canopy act as a functional reserve of minerals such as N. This also may lead to retention of a high P_{max} (Sinclair and Sheehy, 1999; Murchie et al., 2002). Lower leaves contribute

relatively little to grain yield during grain filling (approximately 3% of light interception in leaf 4 at anthesis); thus, optimizing photoacclimation in flag leaf and second leaf will be the main targets for yield potential gains, while leaves 3 and 4 will be the main targets for gains in photosynthetic N use efficiency (PNUE). Although a decline in photosynthesis generally corresponds to the change in light during canopy development, there is variation in this relationship according to species (Hikosaka, 2016). The extent of optimality of photoacclimation (in isolation from other factors) depends on the exact sequence, frequency, and duration of high-light fluctuations of light within the canopy. The latter is unknown for realistic canopy light fluctuations. In other words, is it economically viable for a leaf to acclimate to high light in order to exploit brief periods of high light (Pearcy, 1990)? We define optimality as that condition that results in the highest carbon gain for a given fluctuating light environment.

To address these questions, we have developed two novel techniques: first, a model of photoacclimation that provides a quantitative indicator of carbon gain, predicting optimal maximal photosynthetic capacity levels (P_{max}^{opt}) for a given variable environment (Retkute et al., 2015); and second, a method for the 3D high-resolution reconstruction of plant canopies without the need to parameterize structural models that, with available ray-tracing techniques (Song et al., 2013), can characterize light in every point in the canopy over the course of a day (Pound et al., 2014; Burgess et al., 2015). This allows precise canopy architecture to be considered and a profile of light intensities for any part of the canopy throughout the day to be produced. Here, we use these techniques in combination with manual measurements of photosynthesis to predict the optimal photoacclimation status (to light alone) throughout canopy depth according to the (variable) light environment determined by contrasting canopy architectures. We show that the P_{max} value optimized for light in all leaves in the bottom canopy layers is substantially lower than that measured, an observation that has implications for PNUE of the whole canopy and questions the common assumption that an accumulation of Rubisco at lower canopy positions allows the exploitation of sunflecks.

RESULTS

The Canopy Light Environment

Figure 1 shows an example of the reconstruction process, while Figure 2 shows the final six canopies (three per growth stage) used in this study. The wheat lines selected were the same as those used for a previous study (Burgess et al., 2015) and were chosen due to their contrasting architectural features. The Parent line (cv Ashby) contains more upright leaves, Line 2 (cv 23-74) contains more curled leaves, and Line 1 (cv 32-129) has an intermediate phenotype (for more details on the wheat lines studied, see "Materials and Methods"). Similar features were observed as in Burgess et al. (2015), except for a more curled leaf phenotype of Line 1 relative to the previous year, slightly increased plant height, and altered leaf area index (LAI [leaf area per unit of ground area]; Tables I and II), measured physical plant measurements, and reconstruction LAI values. Burgess et al. (2015) showed that manually measured leaf area corresponded well to reconstructed values. Here, we find that LAI was slightly higher in all the reconstructions compared with the measured values, which was likely due to differences in the way in which stem and leaf area is accounted for in each method. In particular, the manual method did not account for all stem material (some was too large for the leaf area analyzer), and the reconstruction method slightly overestimated stem area. This overestimation was consistent for all lines. Plant density, tillering, and plant height were equivalent in Lines 1 and 2 but slightly higher in the Parent line (Table I). Further architectural characteristics of the three contrasting lines are given in Supplemental Table S1.

Simulations of the light environment within each of the canopies indicate that the daily PPFD decreases with depth in all three plots at both growth stages; however, there is considerable heterogeneity at each depth that needs to be accounted for in the model application. Figure 3 shows how PPFD varies with depth in three randomly selected triangles at each of the three depth positions where samples for Rubisco measurements were taken and where gas-exchange measurements were made. The progressive lowering in the canopy position also leads to more infrequent periods of high light intensity, or sunflecks, interspersed with periods of low light intensity, approaching the critical value for positive net photosynthesis (see below). Similar light signatures are seen for all canopies and both growth stages studied (data not shown). To validate the predicted light levels in each of the canopies using ray tracing, the modeled data were compared with manual measurements taken in the field with a ceptometer as the logarithm of the ratio of light received on a horizontal surface and light intercepted by a point on the leaf (Ln[L/Lo]; Supplemental Fig. S1).

Disparity between Modeled and Measured P_{max} at the Bottom of the Canopy

Figure 4 shows LRCs of photosynthesis for each of the lines at three canopy levels. Typical responses are seen: a decline in both P_{max} and dark respiration rate with increasing canopy depth. A significant lowering of P_{max} was observed within the two lower layers at postanthesis. A comparison of photosynthesis rates with light levels (Fig. 3) shows that all leaves would remain above the light compensation point and positively contribute to carbon gain.

An empirical model of photoacclimation was applied (Retkute et al., 2015; see "Materials and Methods") to

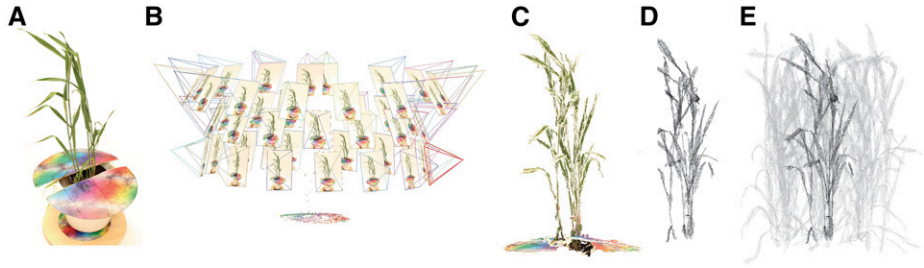

Figure 1. Overview of the reconstruction process. A, Original photograph. B, Point cloud reconstruction using stereocameras (Wu, 2011). C, Output point cloud. D, Mesh following the reconstruction method (Pound et al., 2014). E, Final canopy reconstruction. The multicolored disc in A to C is a calibration target used to optimize the reconstruction process and scale the final reconstructions back to their original units.

predict P_{max}^{opt} for 250 canopy positions. The model includes a time-weighted average (τ), a calculation of the effect of a variable induction state that manifests as a gradually fading memory of a high-light event (see "Modeling" in "Materials and Methods"). The average is applied to the transition from low to high light (but not high to low light) to effectively account for induction state, which is very difficult to measure in situ and not possible for all points in the canopy, as it reflects the past light history of the leaf. Within the main experiment of this study, τ was set at 0.2, which is equivalent to a maximum leaf memory of around 12 min and is in line with previous studies and fit with past experimental data (Pearcy and Seemann, 1990; Retkute et al., 2015). The effect of this time-weighted average is given in Supplemental Figure S2. Figure 5 shows the results of the modeled P_{max}^{opt} against measured P_{max}. Strikingly, the measured P_{max} was substantially higher than predicted, except in the upper parts of the canopy, which showed good correspondence. This was consistently the case for all lines at both growth stages. In the lowest canopy positions (below 300 mm from the ground), the measured values of P_{max} were several times higher than the lowest predicted values: 1 to 2 μmol CO_2 m^{-2} s^{-1}. In these positions, the important features were those that support a positive carbon gain in extremely low-light environments, notably a very low dark respiration level (measured at less than 0.5 μmol m^{-2} s^{-1}) and light compensation point. In other words, the measured P_{max} would rarely be achieved in situ, largely due to the brevity of the high-light periods and the slow induction of photosynthesis.

A comparison with Figure 3 shows that light levels in this part of the canopy were extremely low: 10 to

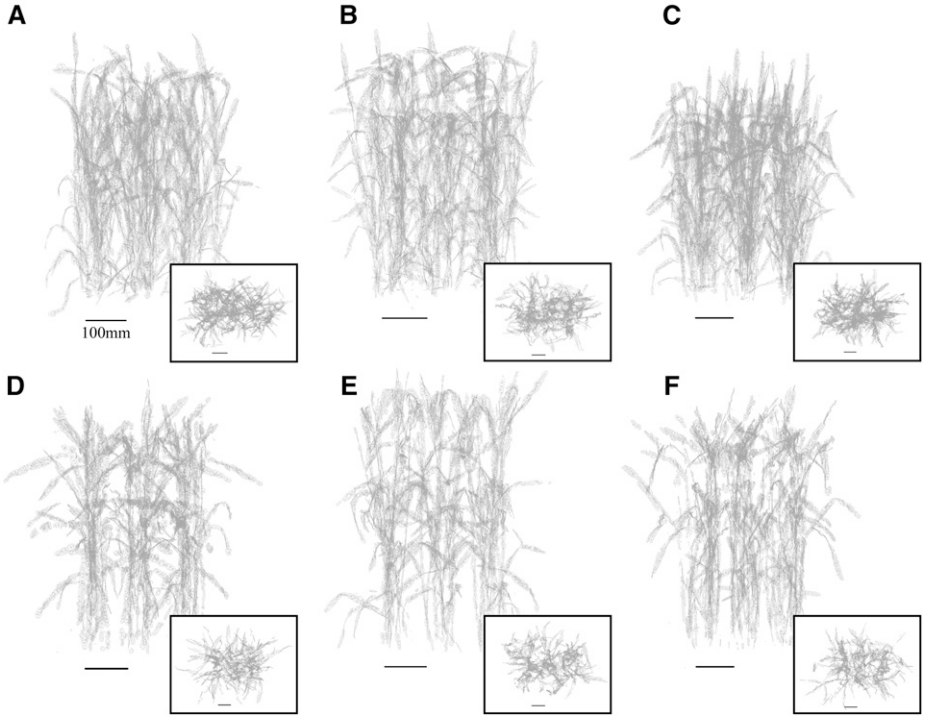

Figure 2. Example canopy reconstructions from front and top-down views. A to C, Preanthesis. D to F, Postanthesis. A and D, Parent line. B and E, Line 1. C and F, Line 2.

Table I. *Physical canopy measurements of each genotype*

The numbers of plants and tillers within a 1-m section along a row at the preanthesis stage were counted and averaged across three plots. The number of shoots for each of the plants used for reconstructions at preanthesis was counted. The resting plant height of five plants per plot was calculated. *P* values correspond to ANOVA. Values are means ± SE; $n = 3$.

Line	Average No. of Plants m^{-1}	Average No. of Shoots m^{-1}	No. of Shoots $Plant^{-1}$	Average Resting Plant Height	
				Preanthesis	Postanthesis
				cm	
Parent	25.3 ± 1.5	69.0 ± 3.1	4.0 ± 0.0	72.1 ± 3.2	84.7 ± 0.3
Line 1	21.3 ± 3.2	61.0 ± 2.3	3.5 ± 0.3	68.3 ± 2.0	90.7 ± 1.6
Line 2	20.7 ± 0.3	62.7 ± 2.7	4.1 ± 0.9	69.5 ± 2.7	94.1 ± 5.5
P	0.287	0.170	0.675	0.579	0.063

30 μmol m^{-2} s^{-1}, punctuated by rare short-lived high-light events with a large variation in frequency and intensity. The decay of modeled P_{max}^{opt} was exponential (Fig. 5), consistent with that of light (Hirose, 2005) and in contrast with the measured P_{max}, which appeared linear. It also was notable that the different canopy architectures (analyzed by Burgess et al. [2015], who used the same set of lines) were associated with a similar disparity between measured and modeled levels of photosynthesis. However, this difference was greater in Line 2 (nonerect leaves), which had a higher rate of light extinction. A comparison of the modeled and measured P_{max} versus PPFD at 12 AM plus modeled P_{max}^{opt} versus daily PPFD is given in Supplemental Figure S3. This shows a similar spread of modeled versus measured P_{max} values and a linear relationship between modeled P_{max}^{opt} and daily PPFD. We also tested the model at a substantially lower value of τ (0.1, equivalent to a leaf memory of 6 min; Supplemental Fig. S4), which results in a more rapid response to light flecks. Even using this parameter, the P_{max} was substantially overestimated in the bottom layer of the canopy. A sensitivity analysis was performed based on the assumption of respiration being proportional to photosynthesis versus respiration having a linear relationship with respect to P_{max} (not allowing dark respiration [Rd] versus Pmax to pass through the origin; see Materials and Methods). First, two lines were fitted to all measured data, and then we varied α by ±10%. In both cases, changes in predicted P_{max} for light patterns at different layers in the canopy changed by less than 9% and could not account for the disparity between modeled and measured data.

Rubisco and Protein Contents Reflect Measured, Not Modeled, Data

During canopy development, wheat leaves will normally emerge into high light and then become progressively more shaded by the production of subsequent leaves. The higher than expected measured P_{max} at the base of the canopy indicates the retention of components of photosynthesis to a level that was excessive when compared with the prevailing light environment. The difference between measured and modeled P_{max} became progressively lower, moving from the bottom of the canopy to the top, until there was complete correspondence at the top of the canopy. Therefore, it is important to confirm the activity of specific components of photosynthesis and compare them with both P_{max} and P_{max}^{opt} values. To understand how Rubisco activity might be changing, we measured ACi (assimilation rate plotted against intercellular CO2 concentration) responses and performed curve fitting to separate the maximum rate of carboxylation (V_{cmax}), electron transport (J), and end product limitation (*Triose-phosphate utilization [TPU]*; Table III). V_{cmax} values at the top of the canopy are consistent with those observed in other studies (Theobald et al., 1998). As we descend the canopy, V_{cmax} declines significantly ($P < 0.05$) in a proportion that is consistent with measured, not modeled, P_{max}. Mesophyll conductance (G_m) was measured

Table II. *Plant and canopy area properties*

Plants were separated into leaf and stem material and measured using a leaf area meter (LI3000C; LI-COR). Measured LAI was calculated as the total area (leaf + stem) divided by the area of ground each plant covered (distance between rows × distance within rows). The reconstructed LAI was calculated as mesh area inside the designated ray-tracing boundaries (see "Imaging and Ray Tracing" in "Materials and Methods"). *P* values correspond to ANOVA. Values are means ± SE; $n = 3$.

Line	Measured ($Plant^{-1}$)				Reconstruction LAI
	Leaf Area	LAI	Total Area	LAI	
Parent	318 ± 20	8.55	799 ± 73	7.22 ± 1.23	8.55
Line 1	312 ± 27	8.39	807 ± 42	6.71 ± 1.30	8.39
Line 2	411 ± 70	9.75	1,118 ± 113	8.78 ± 1.90	9.75
P	0.290	0.167	0.520	0.520	

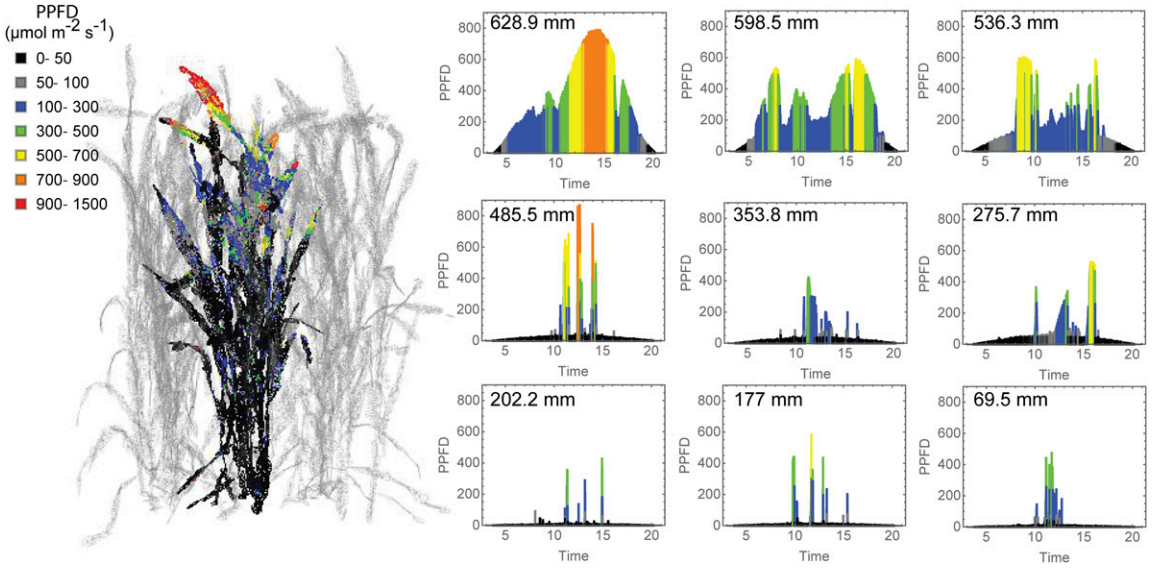

Figure 3. Progressive lowering of the canopy position in a canopy results in the reduction in daily integrated PPFD (μmol m^{-2} s^{-1}) but also in the pattern and incidence of high-light events within the canopy. The left side shows a representative reconstructed preanthesis wheat canopy with a single plant in bold. Maximum PPFD ranges are color coded. The right side shows PPFD during the course of a day at nine representative and progressively lower canopy positions (the height of each canopy location from the ground is given in the top left corner of each graph) calculated using ray-tracing techniques.

but showed no significant differences ($P < 0.05$) between lines or layers.

To analyze photoacclimation further, amounts of Rubisco, total soluble protein (TSP), and chlorophyll were quantified (Table IV). Rubisco amounts at the top of the canopy were consistent with those toward the upper end for wheat (Theobald et al., 1998) and are highly correlated with measured P_{max} and V_{cmax} within the canopy (Fig. 6). This indicates that Rubisco content accounts for all values of measured P_{max} and V_{cmax} but not the modeled P_{max} values. Other work using similar techniques to characterize rice (*Oryza sativa*) canopies came to a similar conclusion (Murchie et al., 2002). Chlorophyll *a*:*b* ratio is a reliable indicator of dynamic photoacclimation (i.e. fully reversible changes occurring at the biochemical level). The changes in chlorophyll *a*:*b* ratio are consistent with those expected for the acclimation of LHCs to a lower light intensity, with the

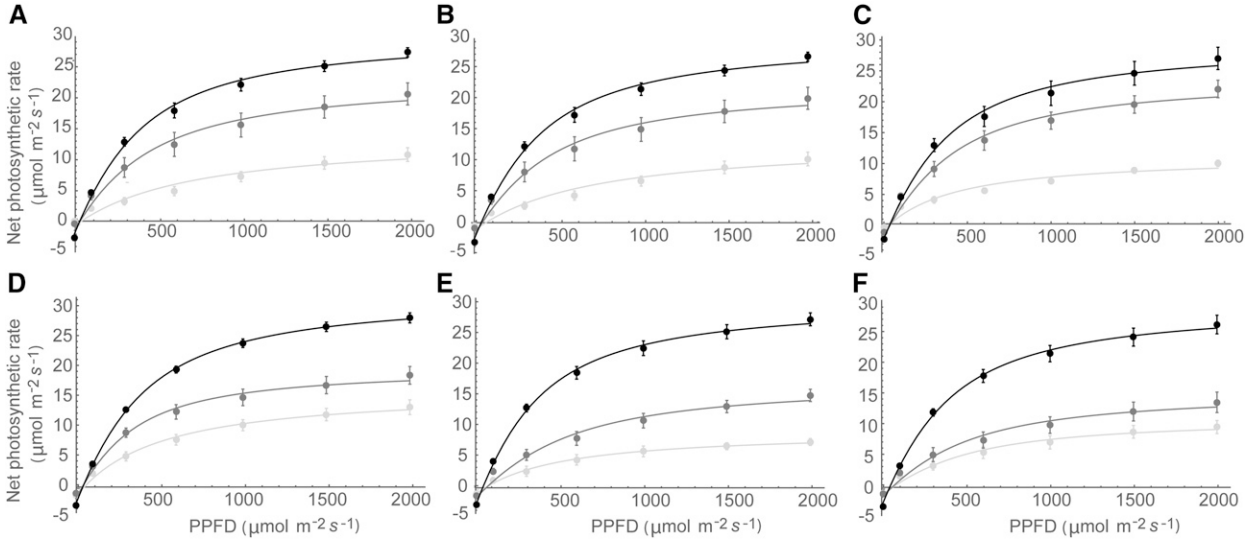

Figure 4. Fitted light response curves (LRCs) for preanthesis in the Parent line (A), Line 1 (B), and Line 2 (C) and for postanthesis in the Parent line (D), Line 1 (E), and Line 2 (F). Layers are top (black), middle (dark gray), and bottom (light gray).

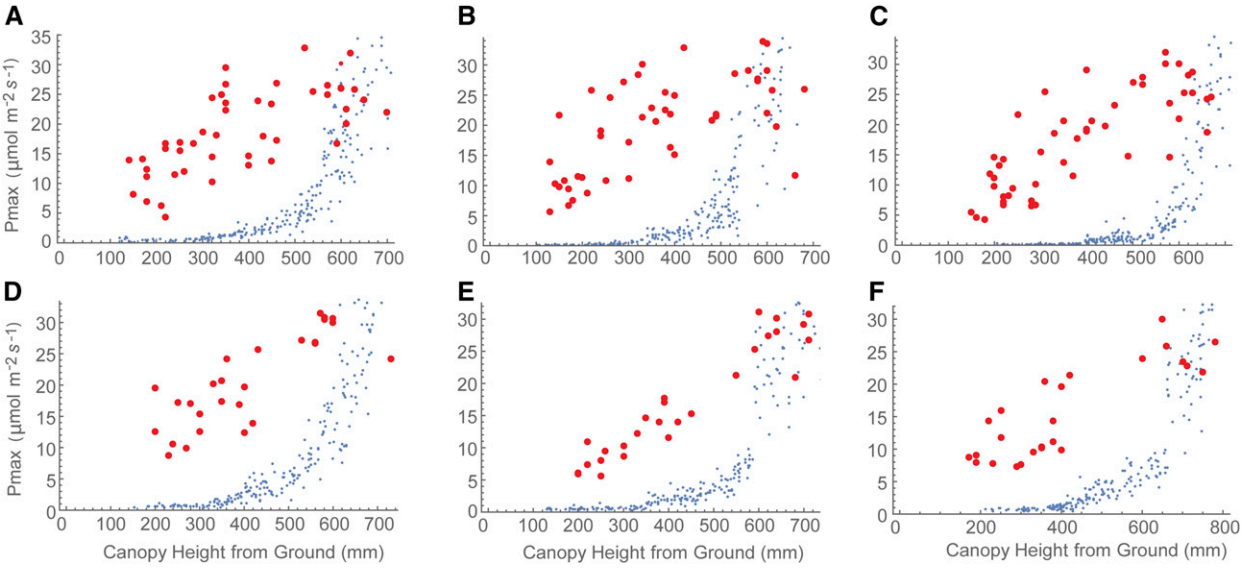

Figure 5. Whole-canopy acclimation model output (blue) versus gas-exchange measurement (red) graphs. The acclimation model was run at 250 locations throughout the canopy depth to predict the optimal P_{max} at each location dependent upon the light environment that it experienced, calculated via ray tracing. The time-weighted average (Eq. 4) was fixed at $\tau = 0.2$. This is an exponentially decaying weight used to represent the fact that photosynthesis is not able to respond instantaneously to a change in irradiance levels. If $\tau = 0$, a plant will be able to respond instantaneously to a change in irradiance, whereas if $\tau > 0$, the time-weighted average light pattern will relax over the time scale τ. Model results are compared with field-measured gas exchange. A to C, Preanthesis. D to F, Postanthesis. A and D, Parent line. B and E, Line 1. C and F, Line 2.

lowered ratio indicating a greater investment in peripheral LHCII (Murchie and Horton, 1997). Interestingly, the largest change in chlorophyll *a*:*b* ratio occurs in the upper half of the canopy, where the greatest proportional change in light level occurs.

DISCUSSION

The regulatory aspects of photoacclimation and how it is triggered by changing light levels are little understood, but recent work has begun to address this and attempt to elucidate the link between variations in light and the resulting biomass and fitness (Külheim et al., 2002; Athanasiou et al., 2010; Retkute et al., 2015; Vialet-Chabrand et al., 2017). In particular, the role of photoacclimation in determining productivity in crop canopies is not known. This study takes a significant first step and reveals, to our knowledge for the first time, the relationship between highly realistic canopy architecture, the resulting dynamic light environment, and its effect on photoacclimation. In addition to a fundamental understanding of photoacclimation, this work has consequences in terms of nutrient usage within our agricultural systems, as discussed below.

Photosynthesis in nature responds largely to fluctuating light, not the unchanging or square waves commonly used for studies in photoacclimation (Poorter et al., 2016; Vialet-Chabrand et al., 2017). The responses of leaves within a wheat canopy were analyzed to predict the optimal state of photoacclimation using light history as a natural dynamic, rather than fixed or artificially fluctuating, parameter. To do this, a framework of image-based 3D canopy reconstruction and ray tracing combined with mathematical modeling was employed to predict the optimal distribution of photosynthetic acclimation states throughout a field-grown wheat canopy based on the realistic dynamic light environment it experiences. The field-measured and modeled data indicate two key features: (1) photosynthesis can vary greatly at the same canopy height according to both photoacclimation and instantaneous irradiance shifts; and (2) while the model indicates good correspondence to field data at the top of the canopy, the model consistently predicts lower optimal P_{max} values in the bottom canopy layers relative to measured data. These predictions are important because they consider the effects of fluctuating light in each layer. We conclude that the high-light events at the base of the canopy are too short and infrequent to represent a substantial carbon resource for crop biomass. From this, we conclude that plants are not optimizing leaf composition in response to the long-term light levels they are experiencing but, rather, are retaining excessive levels of photosynthetic enzymes at lower canopy levels. As discussed below, the latter probably represents an intrinsic influence that could include developmental processes and nutrient remobilization. Regardless of the cause, it also signifies untapped photosynthetic potential and opportunities to improve (photosynthetic) nutrient use efficiency.

Table III. *Parameters taken from curve fitting*

P_{max} was taken from LRCs, and V_{cmax}, *J*, *TPU*, R_d, and G_m were taken from ACi curves (fitting at 25°C; I = 3.74 using Sharkey et al., 2007). Values are means ± SE; $n = 9$ for P_{max} and $n = 5$ for ACi parameters. *P* values correspond to ANOVA.

Time	Line	Layer	P_{max}	V_{cmax}	*J*	*TPU*	R_d	G_m
			$\mu mol\ m^{-2}\ s^{-1}$					$\mu mol\ m^{-2}\ s^{-1}\ Pa^{-1}$
Preanthesis	Parent	Top	30.1 ± 2.2	225 ± 14	305 ± 5	24.0 ± 0.4	5.1 ± 0.5	12.3 ± 7.5
		Middle	25.0 ± 2.0	124 ± 8	232 ± 17	18.2 ± 1.3	3.9 ± 0.7	35.2 ± 7.0
		Bottom	15.6 ± 0.8	80 ± 8	169 ± 16	13.5 ± 1.1	2.1 ± 0.4	37.1 ± 5.1
	Line 1	Top	32.3 ± 0.7	185 ± 19	313 ± 24	24.2 ± 1.9	5.4 ± 1.1	28.1 ± 8.2
		Middle	23.6 ± 1.8	150 ± 37	259 ± 34	19.9 ± 2.9	4.7 ± 1.3	35.0 ± 7.1
		Bottom	12.3 ± 1.4	64 ± 24	103 ± 14	8.3 ± 1.1	3.2 ± 1.1	24.9 ± 10.3
	Line 2	Top	30.3 ± 2.5	200 ± 46	290 ± 24	23.1 ± 2.5	4.2 ± 2.2	37.3 ± 4.9
		Middle	25.8 ± 2.1	111 ± 14	246 ± 25	19.0 ± 1.7	3.3 ± 0.8	34.4 ± 7.8
		Bottom	11.0 ± 0.7	73 ± 13	125 ± 15	10.1 ± 1.2	2.3 ± 0.4	26.1 ± 9.9
	P between lines		0.638	0.733	0.718	0.691	0.380	0.772
	Mean	Top	30.9	203	303	23.7	4.90	25.9
		Middle	24.8	128	246	19.0	3.96	35.0
		Bottom	13.0	73	134	10.8	2.52	29.7
	P between layers		<0.001	<0.001	<0.001	<0.001	0.042	0.351
Postanthesis	Parent	Top	33.8 ± 1.0	154 ± 14	251 ± 25	19.3 ± 2.0	4.1 ± 0.8	12.3 ± 7.5
		Middle	21.9 ± 1.8	111 ± 10	207 ± 20	16.1 ± 1.6	2.7 ± 0.3	26.9 ± 8.7
		Bottom	16.1 ± 1.6	70 ± 30	106 ± 19	8.6 ± 1.4	1.8 ± 0.5	26.5 ± 9.6
	Line 1	Top	32.3 ± 1.3	150 ± 11	253 ± 16	19.8 ± 1.2	2.5 ± 0.5	14.0 ± 7.2
		Middle	17.6 ± 1.4	71 ± 2	132 ± 6	10.3 ± 0.5	1.2 ± 0.2	36.0 ± 6.2
		Bottom	9.6 ± 0.9	31 ± 3	65 ± 7	5.4 ± 0.4	1.3 ± 0.2	28.0 ± 8.6
	Line 2	Top	31.7 ± 1.9	156 ± 22	262 ± 15	20.7 ± 0.9	4.1 ± 0.7	17.8 ± 7.3
		Middle	16.2 ± 1.8	92 ± 15	187 ± 23	14.6 ± 1.7	2.4 ± 0.6	36.7 ± 5.5
		Bottom	9.3 ± 0.8	45 ± 9	90 ± 8	7.5 ± 0.5	1.7 ± 0.3	42.2 ± 0.2
	P between lines		<0.001	0.106	0.027	0.024	0.012	0.009
	Mean	Top	32.6	154	255	20.0	3.58	14.7
		Middle	18.5	92	175	13.7	2.08	33.2
		Bottom	11.7	50	87	7.1	1.60	30.7
	P between layers		<0.001	<0.001	<0.001	<0.001	<0.001	0.330

Influence of Canopy Light Dynamics on Acclimation

Monospecies crop canopies have more consistent structural patterns in comparison with natural systems and are useful models for this type of work, since data can be classified according to stratification but still include spatial complexity and an inherent stochastic component. Photoacclimation according to canopy level is an expected property (Supplemental Fig. S1). The dynamic nature of the in-canopy light environment means that any leaf may be exposed to a range of conditions, from light saturation to light limitation, but

Table IV. *Rubisco, total soluble protein, and chlorophyll contents plus chlorophyll* a:b *and Rubisco: chlorophyll ratios in each layer through the canopy at the postanthesis stage*

Values are means ± SE; $n = 6$. *P* values correspond to ANOVA.

Line	Layer	Rubisco	TSP	Chlorophyll	Chlorophyll *a*:*b*	Rubisco:Chlorophyll
		$g\ m^{-2}$		$mg\ m^{-2}$		
Parent	Top	2.49 ± 0.16	5.35 ± 0.40	844 ± 49	1.93 ± 0.04	2.95 ± 0.11
	Middle	1.36 ± 0.08	2.95 ± 0.12	723 ± 21	1.79 ± 0.03	1.88 ± 0.09
	Bottom	0.98 ± 0.12	2.30 ± 0.27	602 ± 46	1.79 ± 0.02	1.61 ± 0.01
Line 1	Top	2.92 ± 0.16	6.22 ± 0.27	820 ± 28	1.98 ± 0.05	3.58 ± 0.23
	Middle	1.30 ± 0.17	3.02 ± 0.40	667 ± 39	1.79 ± 0.02	1.92 ± 0.15
	Bottom	0.94 ± 0.14	2.04 ± 0.38	532 ± 55	1.68 ± 0.03	1.74 ± 0.16
Line 2	Top	2.29 ± 0.10	5.22 ± 0.26	734 ± 36	1.99 ± 0.04	3.13 ± 0.10
	Middle	1.12 ± 0.07	2.57 ± 0.20	618 ± 20	1.75 ± 0.03	1.81 ± 0.07
	Bottom	0.62 ± 0.07	1.43 ± 0.16	440 ± 51	1.72 ± 0.05	1.41 ± 0.07
P between lines		0.002	0.019	0.002	0.763	0.015
Mean	Top	2.57	5.60	799	1.96	3.22
	Middle	1.26	2.85	669	1.78	1.87
	Bottom	0.85	1.93	525	1.73	1.58
P between layers		<0.001	<0.001	<0.001	<0.001	<0.001

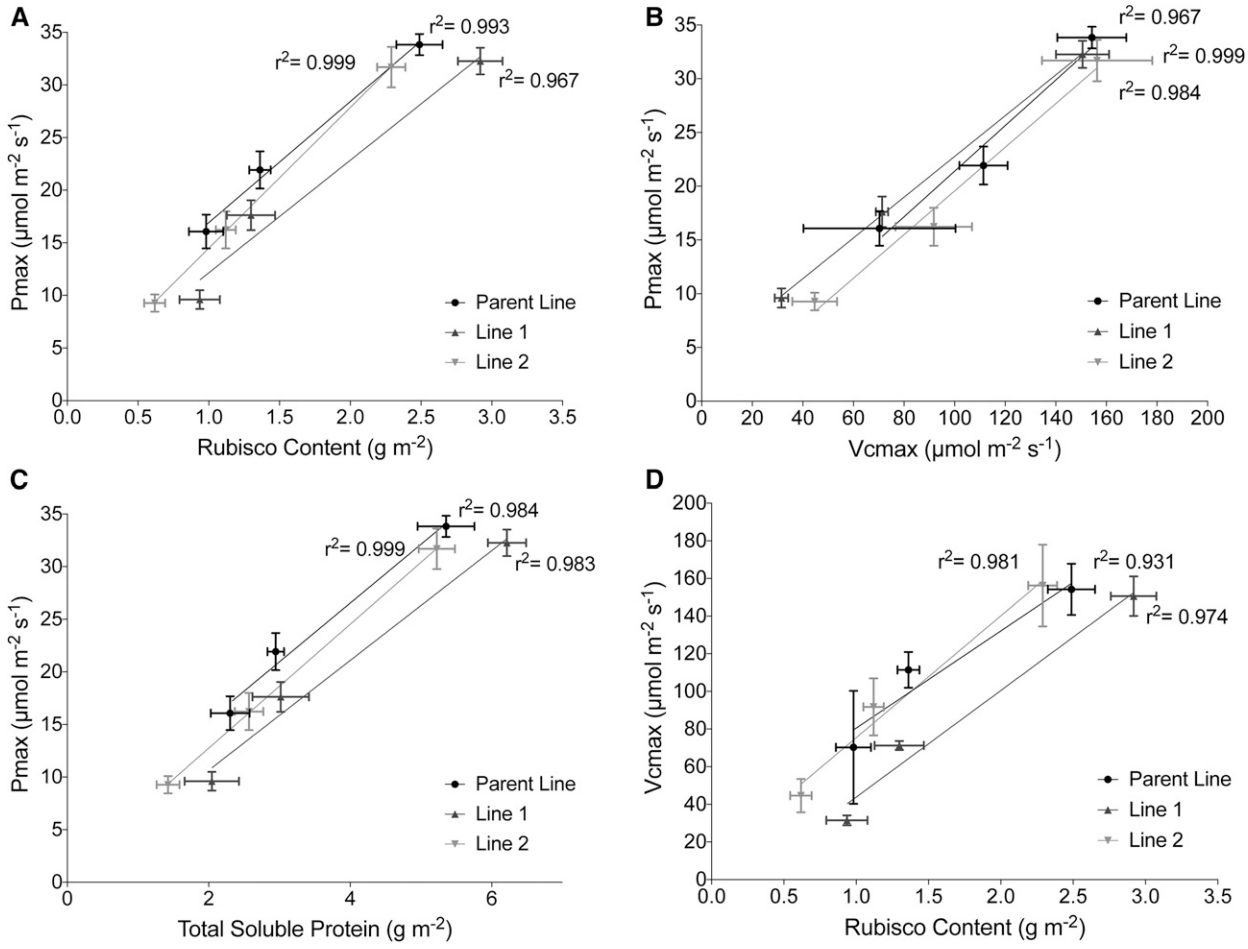

Figure 6. Relationships between photosynthesis (P_{max} taken from fitted LRCs) and Rubisco properties (V_{cmax} from fitted ACi curves and Rubisco/TSP amount) throughout the canopy depth. A, P_{max} and Rubisco content. B, P_{max} and V_{cmax}. C, P_{max} and TSP. D, V_{cmax} and Rubisco content. Black (circles) represents the Parent line, dark gray (triangles) represents Line 1, and light gray (upside-down triangles) represents Line 2.

with varying probability of either according to canopy depth. Figure 3 clearly shows how leaves at the top of the canopy experience high likelihood of direct radiation, with fluctuations ranging from 2- to 3-fold depending on leaf position. Lower in the canopy, occlusion results in an increasing dominance of diffuse and low levels of radiation punctuated by brief and rare high-light events (sunflecks) that can be 10 to 50 times the mean level. Both the measured and modeled canopy light levels indicate that the optimal photosynthesis should be low, based upon the low, basal levels of light the lower canopy layers receive. This is in agreement with the modeled P_{max} values; however, the measured P_{max} values are much higher than this (Fig. 5). The key question, therefore, is whether maintaining higher P_{max} is beneficial and necessary to exploit sunflecks.

Much previous literature has discussed the importance of exploiting sunflecks as a carbon resource in light-limited environments, such as forest understories (Pearcy, 1990), and the role of fluctuating light in determining photosynthesis, for which N profiling in canopies has been discussed (Hikosaka, 2016). However, the response seems to be variable, depending on the physiological acclimation of each species and stresses associated with increased temperatures and high light (Watling et al., 1997; Leakey et al.., 2005). Here, the use of a novel acclimation model allows us to assess the effectiveness of photoacclimation in terms of carbon gain at each position in realistic canopy reconstructions. As sunflecks become rare in the lower portions of the canopy, the model predicts that the acclimation of P_{max} toward higher values becomes an increasingly ineffective strategy in terms of exploiting them for carbon gain. To efficiently exploit the sunflecks in the lower canopy positions, it is necessary to have a high photosynthetic capacity (P_{max}), a rapid rate of photosynthetic induction, and a degree of photoprotective tolerance to avoid photoinhibition. The latter point is not accounted for in this study but has been noted in other species, especially where much higher leaf temperatures are involved (Leakey et al., 2005).

Photoinhibition (maximum quantum yield in the dark-adapted state lower than 0.8) in lower parts of wheat canopies in the United Kingdom was not observed in this study (data not shown) or in a previous study (Burgess et al., 2015), and in our temperate system, we do not expect excessive leaf temperatures. It is possible that the high P_{max} observed in lower layers of the canopy helps to prevent excessive photoinhibition. Photosynthetic induction state is determined by the previous light history of the leaf, by stomatal dynamics, and by the activation state of key enzymes such as Rubisco. The acclimation of P_{max} becomes more effective in terms of overall carbon gain where there is a lower frequency of light transitions but increasing duration of high-light events (Retkute et al., 2015). This is consistent with the light data (Fig. 3), which show rare, brief high-light events lower in the wheat canopy.

Such very low levels of light within a crop canopy are comparable with forest floors, where morphological and molecular adaptations are used to enhance light harvesting, carbon gain, and avoid photoinhibition during high-light periods (Powles and Björkman, 1981; Raven, 1994; Sheue et al., 2015). The interesting feature of cereal canopy development is the fact that leaves initially develop in high light and then are shaded progressively as the canopy matures. Since the morphology of the leaf is determined prior to emergence, all acclimation to low light, post emergence, must be at the biochemical level, as shown by the chlorophyll *a*:*b* ratio (Murchie et al., 2005). The low light levels within the wheat canopy also require effective acclimation of respiration rates to maintain positive carbon gain, and this was observed here (Fig. 4). Leaf respiration is a critical aspect of photoacclimation, permitting lowered light compensation points and positive carbon balance in low light. The relatively low rates of dark respiration in the lower layers and the very low measured light levels at the base of the canopy indicate that leaves maintain their (measured) high P_{max} alongside low respiration rates and light compensation points. Therefore, there must be some decoupling of P_{max} from these other photoacclimation processes at lower light levels. The importance of R_d should be stated here, due to its importance in derivation of the term α and for confirmation that the same relationship between R_d and α holds regardless of the nature of the fluctuating light environment. However, first, improvements must be made for the accurate measurement of R_d. This also would allow for detailed studies on the acclimation of R_d to a change in light levels.

We conclude, perhaps surprisingly, that the optimal strategy in lower parts of the wheat canopy where light is extremely low (less than 50 μmol m^{-2} s^{-1}) should be geared not toward exploiting sunflecks (seen previously as an important carbon resource) but toward light harvesting and the maintenance of low leaf respiration and low light compensation point. Indeed, the photoacclimation of P_{max} to higher levels requires substantial investments of resources such as energy, N, and carbon. It is still possible that the high measured P_{max} may allow a greater ability to exploit some sunflecks of increased duration where they do not lead to substantial photoinhibition (Raven, 2011). It is likely that the planting density has an effect: in this experiment, we used standard sowing rates for the United Kingdom, where the LAI is reasonably high, leading to a dense canopy. The excessive accumulation of Rubisco in lower leaves may be more useful for exploiting light in planting systems where spacing is greater and light penetration is higher (Parry et al., 2011). There is little genetic variation for P_{max}, respiration rate, and light compensation point in the three lines presented here (Fig. 4), although ongoing research is aimed at identifying further sources of genetic variation for improving these traits (Parry et al., 2011; Reynolds et al., 2012). Future studies also will need to focus on enhancing photoacclimation in flag leaf and L2.

Implications in Terms of Nutrient Budgeting

The disparity between modeled data and manually measured data has consequences in terms of the canopy nutrient budget. Photosynthetic components are a significant sink for leaf N: chloroplasts account for up to 80% of total leaf N, with Rubisco being the dominant enzyme (Evans, 1989; Makino and Osmond, 1991; Theobald et al., 1998). Higher photosynthetic capacity, therefore, requires a higher N (Evans and Terashima, 1987; Terashima and Evans, 1988; Verhoeven et al., 1997; Evans and Poorter, 2001; Terashima et al., 2005; Niinemets and Anten, 2009). Photoacclimation to high irradiance often is associated with an increase in the synthesis of Rubisco per unit of leaf area (Evans and Terashima, 1987); therefore, PNUE will remain high only if the high irradiance is sustained. The decay of light within plant canopies commonly results in a correlation between the distribution of photosynthetic capacity, light, and specific leaf N (Anten et al., 1995; de Pury and Farquhar, 1997; Hikosaka, 2016). However, in real canopies, the correlation often is not linear, leading to the conclusion that the relationship is suboptimal, either as an overaccumulation of N in lower regions of the canopy or an inability to photoacclimate to higher light (Buckley et al., 2013; Hikosaka, 2016). There appears to be species variation within these relationships: a recent meta-analysis showed that the N extinction coefficient for wheat was determined by LAI alone, whereas, in other species it was codetermined by the light extinction coefficient (Moreau et al., 2012; Hikosaka, 2016). In the literature, many other reasons have been given for this lack of correspondence, including herbivory and stomatal and mesophyll limitation (Hikosaka, 2016). The novelty of our work is the extent of disparity between predicted and optimal P_{max} at most canopy levels.

Wheat plants and other cereals exhibit a pattern of storage of N in leaves, leaf sheaths, and stems prior to grain filling, whereby a substantial proportion of stored N is remobilized toward the grain, where it contributes

to protein synthesis (Foulkes and Murchie, 2011; Gaju et al., 2011; Moreau et al., 2012). For bread wheat, this is especially important for grain quality. Similar mechanisms occur in many plant species to conserve nutrients; therefore, the retention of N in leaves represents a strategy for storage in the latter part of the plant's life. Since wheat leaves develop in high light and become progressively shaded, their net lifetime contribution to canopy photosynthesis within the shaded environment will still be substantial. This secondary property of photosynthetic enzymes for N storage has been discussed previously (Sinclair and Sheehy, 1999). It is clear that this role is valid, but it is still not certain how it is coordinated effectively with photosynthetic productivity, since remobilization and subsequent senescence represent a compromise to canopy carbon gain in the latter grain-filling periods. In this case, it is clear that the accumulation and retention of N in lower leaves of the wheat canopy are dominant over the regulation of key components of optimal photoacclimation, especially P_{max}, and it is doubtful whether the excess N is used to promote carbon gain at the canopy level. The mechanism for this partitioning strategy is not known: it is still possible that the metabolic cost of removing the leaf N is simply greater than the cost of retaining it in the leaves. Were this to be the case, then it implies a high degree of precision of the leaf photoacclimation process that is linked to whole-plant metabolism. Therefore, questions must be raised regarding the cost of this accumulation and whether all N is efficiently remobilized to improve grain quality. Recent data for UK wheat show that only 76% of leaf N is remobilized, indicating that a substantial improvement in nutrient use efficiency could be achieved with no penalty for photosynthesis or grain quality (Pask et al., 2012). However, this value is even lower for other plant components, with only 48% of N stored in the stem and 61% stored in the leaf sheath remobilized to the grain (Pask et al., 2012). Altering the photoacclimation responses of the lower leaves to fluctuating light could bring about this improvement.

Cross-species correlations between leaf N content and dark respiration have been observed, raising a further question over the respiratory cost of accumulating leaf N in such low-light levels, where the opportunities to exploit sunflecks are not high and are not warranted in terms of photoacclimation of P_{max} (Reich et al.,1998). Sinclair and Sheehy (1999) pointed out that the erect nature of rice leaves had an important effect in terms of improving the capacity of the lower leaves to store N for remobilization. Furthermore, we suggest that even small changes in canopy architecture or physical properties (Burgess et al., 2015, 2016) would permit lower leaves to operate more efficiently as N storage organs in addition to their role as net carbon contributors.

CONCLUSION

Photosynthetic acclimation permits photosynthesis to optimize to the prevailing light conditions, but its regulation in natural fluctuating light is poorly understood. Here, we show that the accumulation of excessive photosynthetic capacity does not, in fact, allow the exploitation of sunflecks for enhanced carbon gain and is not optimal for exploiting the wheat canopy light environment, as revealed by high-resolution 3D reconstruction methods. This observation has some profound implications for the improvement of canopy photosynthesis and resource use efficiency in crops. First, the unused photosynthetic potential in lower parts of the canopy (which can be achieved without the addition of extra nutrients) could be used to enhance biomass and grain yield through increasing light penetration and reducing the inherent plant-plant competition. This can be achieved by previously published routes, such as architecture (Burgess et al., 2015), by altering the distribution of chlorophyll content (Zhu et al., 2010; Ort et al., 2011), and/or by manipulating mechanical properties to optimize movement in response to low wind levels (Burgess et al., 2016). Second, there is an opportunity to improve photosynthetic nutrient use efficiency: we have shown that levels of canopy nutrients (especially N) could be reduced with no detrimental impact on either carbon gain or grain protein content.

MATERIALS AND METHODS

Plant Material

Wheat (*Triticum aestivum*) lines with contrasting canopy architectures were selected from an ongoing field trial at the University of Nottingham farm (Sutton Bonington Campus) in Leicestershire, United Kingdom (52.834 N, 1.243 W), on a sandy loam soil type (Dunnington Heath Series) in 2015. A total of 138 double haploid lines were developed jointly by the University of Nottingham and the Internation Maize and Wheat Improvement Center (CIMMYT) between the CIMMYT large ear phenotype spring wheat advanced line LSP2 and UK winter wheat cv Rialto, as described by Burgess et al. (2015). This approach resulted in the formation of a large number of stable lines with contrasting canopy architecture but with values of light-saturated photosynthesis consistent with previous published measurements for field-grown wheat in the United Kingdom (Driever et al., 2014; Gaju et al., 2016). Two double haploid lines were then selected, and each was backcrossed three times with the UK spring wheat cv Ashby to produce BC_3 plants. The BC_3 lines were selected phenotypically to contrast for tillering and canopy architecture phenotypes. The BC_3 lines were then selfed for five generations before bulking seed of BC_3S_5 plants for this trial. Three wheat lines were used for analysis: cv Ashby (the recurrent Parent line) and two BC_3 lines, cv 32-129 (Line 1) and cv 23-74 (Line 2). This resulted in lines that were well adapted to the UK environment but that provided contrasts for canopy architecture.

The experiment used a completely randomized block design with three replicates. The plot size was 6×1.65 m, and the sowing date was October 20, 2014. Previous cropping was winter oilseed rape (*Brassica napus*). The field was plowed and power harrowed and rolled after drilling. The seed rate was adjusted by genotype according to 1,000 grain weight to achieve a target seed rate of 300 seeds m^{-2}; rows were 0.13 m apart. A total of 192 kg ha^{-1} N fertilizer as ammonium nitrate was applied in a three-split program. P and K fertilizers were applied to ensure that these nutrients were not limiting. Plant growth regulator was applied at GS31 to reduce the risk of lodging. Herbicides, fungicides, and pesticides were applied as required to minimize the effects of weeds, diseases, and pests. Two growth stages were analyzed: preanthesis and postanthesis (equivalent to GS55–GS71; Zadoks et al.., 1974).

Plant Physical Measurements

Physical measurements were made on plants in the field (Table I; Supplemental Table S1). The number of plants and shoots within a 1-m section

along the middle of each row was counted and averaged across the three replicate plots. This average value was used to calculate the planting density within the plots and, thus, to ensure that the reconstructed canopies were representative of field conditions. Plant dry weight and area (excluding ears) were analyzed by separating shoot material into stem and leaf sheath, flag leaf lamina, and all other leaf lamina before passing them through a leaf area meter (LI3000C; LI-COR) for six replicate plants (two per plot; those used for the reconstruction of canopies below). Each component was then dried individually in an oven at 80°C for 48 h or until no more weight loss was noted. Plants were weighed immediately. Measured LAI (leaf area per unit of ground area; m^2) was calculated as the total area (leaf + stem) divided by the area of ground each plant covered (distance between rows × distance within rows) and averaged across the six replicate plants.

Imaging and Ray Tracing

3D analysis of plants was made according to the protocol of Pound et al. (2014), and further details are given by Burgess et al. (2015). An overview of this process is given in Figure 1. From the sampled and reconstructed plants, canopies were made in silico according to Burgess et al. (2015). Two replicate plants representative of the morphology of each wheat line were taken per plot, giving six replicates per line, and reconstructed; at least four of these were used to form each of the final canopies (Fig. 2). The wheat ears (present postanthesis) were removed manually from the resultant mesh, as the reconstructing method is unable to accurately represent their form. Reconstructed canopies were formed by duplicating and randomly rotating the plants in a 3 × 4 grid, with 13 cm between rows and 5 cm within rows (calculated from field measurements). The LAI of each reconstructed canopy was calculated as the area of mesh inside the ray-tracing boundaries divided by the ground area. The LAI of the plots was then compared with the LAI for each of the reconstruction plots (Table II). Total light per unit of leaf area was predicted using a forward ray-tracing algorithm implemented in fastTracer version 3 (PICB; Song et al., 2013). Latitude was set at 53 (for Sutton Bonington), atmospheric transmittance at 0.5, light reflectance at 7.5%, and light transmittance at 7.5%; days 155 and 185 (June 4 and July 4: preanthesis and postanthesis, respectively) were sampled. fastTracer version 3 calculates light as direct, diffused, and transmitted components separately; these were combined to give single irradiance levels for all canopy positions. The diurnal course of light intensities over a whole canopy was recorded in 1-min intervals. The ray-tracing boundaries were positioned within the outside plants to reduce boundary effects. To validate the light interception predicted by ray tracing, fractional interception was calculated at different depths throughout the field-grown wheat canopies using a ceptometer (AccuPAR). Light levels at the top, three-quarters, half, one-quarter, and bottom of the plant canopies were taken. Five replicates were taken per plot. This was compared with fractional interception calculated from ray tracing (Supplemental Fig. S1).

Gas Exchange and Fluorescence

Measurements were made on field-grown wheat in plots in the same week in which the plants were imaged. For LRCs and ACi response curves of photosynthesis, leaves were not dark adapted. Leaf gas-exchange measurements (LRC and ACi) were taken with a LI-COR 6400XT infrared gas-exchange analyzer. The block temperature was maintained at 20°C using a flow rate of 500 mL min^{-1}. Ambient field humidity was used. LRCs were measured over a series of seven photosynthetically active radiation values between 0 and 2,000 μmol m^{-2} s^{-1}, with a minimum of 2 min and a maximum of 3 min at each light level moving from low to high. LRCs were measured at three different canopy heights, labeled top (flag leaf), middle, and bottom, with height above the ground being noted. Three replicates were taken per treatment plot per layer, thus leading to nine replicates per line. Saturation of photosynthesis was verified for each light response step by conducting a separate set of LRCs where photosynthesis was logged every few seconds. It was verified that this protocol resulted in saturation at each light level. For the ACi curves, leaves were exposed to 1,500 μmol m^{-2} s^{-1}. They were placed in the chamber at 400 μL L^{-1} CO_2 for a maximum of 2 min, and then CO_2 was reduced stepwise to 40 μL L^{-1} and then increased to 1,500 μL L^{-1}, again in a stepwise manner. At least one replicate was taken per treatment plot per layer, but with five replicates taken for each of the three lines. Individual ACi curves were fitted using the tool described by Sharkey et al. (2007), with leaf temperature set at 20°C, atmospheric pressure at 101 kPa, oxygen pressure at 21 kPa, and limiting factors assigned as suggested by Sharkey et al. (2007). A Walz MiniPam fluorometer was used to measure dark-adapted values of maximum photochemical efficiency of PSII in the field wheat every hour between 9 AM and 5 PM. Dark adaptation for 20 min was applied using the method of Burgess et al. (2015). Four replicates were taken per plot per layer. Measurements were not taken for the bottom layer.

Rubisco Quantification

Leaf samples were taken from the same leaves and the same region of the leaf as the gas-exchange measurements. One day was left between gas exchange and sampling. Leaf samples (1.26 cm^2) were ground at 4°C in an ice-cold pestle and mortar containing 0.5 mL of 50 mM Bicine-NaOH, pH 8.2, 20 mM $MgCl_2$, 1 mM EDTA, 2 mM benzamidine, 5 mM ε-aminocaproic acid, 50 mM 2-mercaptoethanol, 10 mM DTT, 1 mM phenylmethylsulfonyl fluoride, and 1% (v/v) protease inhibitor cocktail (Sigma-Aldrich). The homogenate was clarified by centrifugation at 14,700*g* and 4°C for 3 min. Rubisco in 150 μL of the supernatant was quantified by the [^{14}C]CABP binding assay (Parry et al., 1997), as described previously (Carmo-Silva et al., 2010). The radioactivity due to [^{14}C]CABP bound to Rubisco catalytic sites was measured by liquid scintillation counting (PerkinElmer). Total soluble protein content in the supernatants was determined by the method of Bradford (1976) using bovine serum albumin as a standard. Chlorophylls in 20 μL of the homogenate (prior to centrifugation) were extracted in 95% (v/v) ethanol for 4 to 8 h in darkness (Lichtenthaler, 1987). After clarifying the ethanol-extracted samples by centrifugation at 14,000*g* for 3 min, the absorbance of chlorophylls in ethanol was measured at 649 and 665 nm. Chlorophyll *a* and *b* contents were estimated using the formulas $C_a = (13.36 \times A_{664}) - (5.19 \times A_{649})$ and $C_b = (27.43 \times A_{649}) - (8.12 \times A_{664})$.

Modeling

All modeling was carried out using Mathematica (Wolfram) using the techniques described in more detail by Retkute et al. (2015) and Burgess et al. (2015). The acclimation model, here adopted for use in the canopy setting, was developed originally based on the observation that Arabidopsis (*Arabidopsis thaliana*) plants subject to a fluctuating light pattern exhibit a higher P_{max} than plants grown under a constant light pattern of the same average irradiance (Yin and Johnson, 2000; Athanasiou et al., 2010). The main model assumption is that plants will adjust P_{max} from a range of possible values in such a way as to produce the largest amount of daily carbon gain. The model predicts P_{max}^{opt} for a given light pattern from LRC parameters (ϕ, θ, and α; explained below).

In this study, we sought to predict P_{max}^{opt} as the P_{max} that represents maximal carbon gain at a single point within the canopy, based on the light pattern that point has experienced (i.e. using the light pattern output from ray tracing; Fig. 3, right). This was predicted across 250 canopy points, thus leading to the distribution of P_{max}^{opt} values throughout each of the canopies. These 250 canopy positions (triangles) from each of the canopies were chosen as a subset of triangles that were of similar size (i.e. area) and constitute a representative sample distribution throughout the canopy depth.

The net photosynthetic rate, P, as a function of PPFD, L, and P_{max} was calculated using the nonrectangular hyperbola:

$$F_{NRH}(L, \phi, \theta, P_{max}, \alpha) = \frac{\phi\ L + (1+\alpha)P_{max} - \sqrt{(\phi L + (1+\alpha)P_{max})^2 - 4\theta\phi L(1+\alpha)P_{max}}}{2\theta} - \alpha P_{max} \quad (1)$$

where L is the PPFD incident on a leaf (μmol m^{-2} s^{-1}), ϕ is the quantum use efficiency, θ is the convexity, and α corresponds to the fraction of P_{max} used for dark respiration according to the relationship $R_d = \alpha\ P_{max}$ (Givnish, 1988; Niinemets and Tenhunen, 1997; Retkute et al., 2015). The value of α was obtained from the LRCs recorded in the field by fitting a line of best fit between measured P_{max} and R_d values for all individual plants ($n > 20$ plants for each wheat line and stage). Therefore, the relationship between P_{max} and R_d used in modeling is based on observation rather than on the assumption of linear fit. All other parameters (e.g. P_{max}, ϕ, and θ) were estimated from the LRCs for three canopy layers using the Mathematica command FindFit.

As each canopy was divided into three layers, each triangle from the digital plant reconstruction was assigned to a particular layer, m, according to the triangle center (i.e. with the triangle center between the upper and lower limits of a layer depth). For each depth (d; the distance from the highest point of the canopy), we found all triangles with centers lying above d:

$$d_i = \max_{j=1,2,3;1 \le i \le n} z_i^j - \left(z_i^1 + z_i^2 + z_i^3\right) \Big/ 3 \quad (2)$$

Each triangle within a specific layer was assigned the LRC parameters from the corresponding measured data.

Carbon gain, C (mol m^{-2}), was calculated over the time period t e $[0,T]$:

$$C(L(t), P_{max}) = \int_0^T P(L(t), P_{max})dt \quad (3)$$

Experimental data indicate that the response of photosynthesis to a change in irradiance is not instantaneous; thus, to incorporate this into the model, Retkute et al. (2015) introduced a time-weighted average for light:

$$L_\tau(t) = \frac{1}{\tau}\int_{-\infty}^{t} L(t')e^{-(t-t')/\tau}dt' \quad (4)$$

This effectively accounts for photosynthetic induction state, which is very hard to quantify in situ, as it varies according to the light history of the leaf. The more time recently spent in high light, the faster the induction response. The time-weighted average effectively acts as a fading memory of the recent light pattern and uses an exponentially decaying weight. If $\tau = 0$, then a plant will be able to respond instantaneously to a change in irradiance, whereas if $\tau > 0$, the time-weighted average light pattern will relax over the time scale τ. In this study, τ was fixed at 0.2 (unless stated otherwise), in agreement with previous studies, and fit with past experimental data (Pearcy and Seemann, 1990, Retkute et al., 2015). The time-weighted average applies only to the transition from low to high light. From high to low light, the response is here considered to be virtually instantaneous and the time-weighted average is not applied. The effect of this decaying weight effectively acts as a filter for irradiance levels, with photosynthesis as slow to respond from a transition from low to high light but quick to respond following a drop in irradiance. This can be seen in Supplemental Figure S3. The value of τ (0.2) selected here represents a maximum leaf memory of around 12 min that declines exponentially according to time spent in the light. We verified this experimentally using wheat leaves grown under irradiance levels that correspond to mid to upper canopy levels: induction from darkness to 1,000 μmol m^{-2} s^{-1} typically took 10 to 20 min to reach the steady-state rate. We also tested the model at a lower value of τ (0.1) to account for leaves capable of faster induction or a longer memory (Supplemental Fig. S4).

Supplemental Data

The following supplemental materials are available.

Supplemental Figure S1. Experimental validation of the predicted light levels.

Supplemental Figure S2. Example of a time-weighted light pattern at τ = 0.2 relative to a nonweighted line.

Supplemental Figure S3. Model output versus gas-exchange measurement graphs for the Parent line preanthesis.

Supplemental Figure S4. Whole-canopy acclimation model output versus gas-exchange measurement graphs.

Supplemental Table S1. Plant physiological measurements (plant height and leaf dimensions) preanthesis.

ACKNOWLEDGMENTS

We thank Xinguang Zhu and Dr. Qinfeng Song (Shanghai Institute for Biological Sciences) for useful input concerning the ray tracer and the following for useful discussions: Martin Parry (Lancaster University), Dr. Mike Pound (University of Nottingham), Tony Pridmore (University of Nottingham), Dr. Simon Preston (University of Nottingham), Dr. Ian Smillie (LI-COR), and Oliver Jensen (University of Manchester). We thank Dr. Peter Werner (KWS) for developing the BC_3 lines.

Received August 31, 2017; accepted December 4, 2017; published December 7, 2017.

LITERATURE CITED

Anderson JM, Chow WS, Park YI (1995) The grand design of photosynthesis: acclimation of the photosynthetic apparatus to environmental cues. Photosynth Res **46:** 129–139

Anderson JM, Osmund CB (1987) Shade-sun responses: compromises between acclimation and photoinhibition. *In* DJ Kyle, CB Osmond, CJ Arntzen, eds, Photoinhibition. Elsevier Science, Amsterdam, pp 1–38

Anten NP, Schieving F, Werger MJ (1995) Patterns of light and nitrogen distribution in relation to whole canopy carbon gain in C_3 and C_4 mono- and dicotyledonous species. Oecologia **101:** 504–513

Athanasiou K, Dyson BC, Webster RE, Johnson GN (2010) Dynamic acclimation of photosynthesis increases plant fitness in changing environments. Plant Physiol **152:** 366–373

Björkman O (1981) Responses to different quantum flux densities. *In* OL Lange, PS Nobel, CB Osmond, H Ziegler, eds, Physiological Plant Ecology. Springer, Berlin, pp 57–107

Bradford MM (1976) A rapid and sensitive method for the quantitation of microgram quantities of protein utilizing the principle of protein-dye binding. Anal Biochem **72:** 248–254

Buckley TN, Cescatti A, Farquhar GD (2013) What does optimization theory actually predict about crown profiles of photosynthetic capacity when models incorporate greater realism? Plant Cell Environ **36:** 1547–1563

Burgess AJ, Retkute R, Pound MP, Preston SP, Pridmore TP, Foulkes MJ, Jensen OE, Murchie EH (2015) High-resolution three-dimensional structural data quantify the impact of photoinhibition on long-term carbon gain in wheat canopies in the field. Plant Physiol **169:** 1192–1204

Burgess AJ, Retkute R, Preston SP, Jensen OE, Pound MP, Pridmore TP, Murchie EH (2016) The 4-dimensional plant: effects of wind-induced canopy movement on light fluctuations and photosynthesis. Front Plant Sci **7:** 1392

Carmo-Silva AE, Keys AJ, Andralojc PJ, Powers SJ, Arrabaça MC, Parry MAJ (2010) Rubisco activities, properties, and regulation in three different C4 grasses under drought. J Exp Bot **61:** 2355–2366

Carmo-Silva AE, Salvucci ME (2013) The regulatory properties of Rubisco activase differ among species and affect photosynthetic induction during light transitions. Plant Physiol **161:** 1645–1655

Chabot BF, Jurik TW, Chabot JF (1979) Influence of instantaneous and integrated light-flux density on leaf anatomy and photosynthesis. Am J Bot **66:** 940–945

de Pury DGG, Farquhar GD (1997) Simple scaling of photosynthesis from leaves to canopies without the errors of big-leaf models. Plant Cell Environ **20:** 537–557

Driever SM, Lawson T, Andralojc PJ, Raines CA, Parry MA (2014) Natural variation in photosynthetic capacity, growth, and yield in 64 field-grown wheat genotypes. J Exp Bot **65:** 4959–4973

Evans JR (1989) Photosynthesis and nitrogen relationships in leaves of C_3 plants. Oecologia **78:** 9–19

Evans JR, Poorter H (2001) Photosynthetic acclimation of plants to growth irradiance: the relative importance of specific leaf area and nitrogen partitioning in maximizing carbon gain. Plant Cell Environ **24:** 755–767

Evans JR, Terashima I (1987) Effects of nitrogen nutrition on electron transport components and photosynthesis in spinach. Funct Plant Biol **14:** 59–68

Foulkes MJ, Murchie EH (2011) Optimizing canopy physiology traits to improve the nutrient use efficiency of crops. *In* MJ Hawkesford, P Barraclough, eds, The Molecular and Physiological Basis of Nutrient Use Efficiency in Crops. Wiley-Blackwell, Chichester, UK, pp 65–83

Gaju O, Allard V, Martre P, Snape JW, Heumez E, LeGouis J, Moreau D, Bogard M, Griffiths S, Orford S, et al (2011) Identification of traits to improve the nitrogen-use efficiency of wheat genotypes. Field Crops Res **123:** 139–152

Gaju O, DeSilva J, Carvalho P, Hawkesford MJ, Griffiths S, Greenland A, Foulkes MJ (2016) Leaf photosynthesis and associations with grain yield, biomass and nitrogen-use efficiency in landraces, synthetic-derived lines and cultivars in wheat. Field Crops Res **193:** 1–15

Givnish TJ (1988) Adaptation to sun and shade: a whole-plant perspective. Funct Plant Biol **15:** 63–92

Hikosaka K (2016) Optimality of nitrogen distribution among leaves in plant canopies. J Plant Res **129:** 299–311

Hirose T (2005) Development of the Monsi-Saeki theory on canopy structure and function. Ann Bot **95:** 483–494

Hubbart S, Ajigboye OO, Horton P, Murchie EH (2012) The photoprotective protein PsbS exerts control over CO_2 assimilation rate in fluctuating light in rice. Plant J **71:** 402–412

Kromdijk J, Głowacka K, Leonelli L, Gabilly ST, Iwai M, Niyogi KK, Long SP (2016) Improving photosynthesis and crop productivity by accelerating recovery from photoprotection. Science **354:** 857–861

Külheim C, Agren J, Jansson S (2002) Rapid regulation of light harvesting and plant fitness in the field. Science **297:** 91–93

Lawson T, Blatt MR (2014) Stomatal size, speed, and responsiveness impact on photosynthesis and water use efficiency. Plant Physiol **164:** 1556–1570

Leakey ADB, Scholes JD, Press MC (2005) Physiological and ecological significance of sunflecks for dipterocarp seedlings. J Exp Bot **56:** 469–482

Lichtenthaler HK (1987) Chlorophylls and carotenoids, the pigments of photosynthetic biomembranes. Methods Enzymol **148:** 350–382

Makino A, Osmond B (1991) Effects of nitrogen nutrition on nitrogen partitioning between chloroplasts and mitochondria in pea and wheat. Plant Physiol **96:** 355–362

Moreau D, Allard V, Gaju O, Le Gouis J, Foulkes MJ, Martre P (2012) Acclimation of leaf nitrogen to vertical light gradient at anthesis in wheat is a whole-plant process that scales with the size of the canopy. Plant Physiol **160:** 1479–1490

Murchie EH, Horton P (1997) Acclimation of photosynthesis to irradiance and spectral quality in British plant species: chlorophyll content, photosynthetic capacity and habitat preference. Plant Cell Environ **20:** 438–448

Murchie EH, Hubbart S, Chen Y, Peng S, Horton P (2002) Acclimation of rice photosynthesis to irradiance under field conditions. Plant Physiol **130:** 1999–2010

Murchie EH, Hubbart S, Peng S, Horton P (2005) Acclimation of photosynthesis to high irradiance in rice: gene expression and interactions with leaf development. J Exp Bot **56:** 449–460

Murchie EH, Reynolds MP (2012) Crop radiation capture and use efficiency. *In* RA Meyers, eds, Encyclopedia of Sustainability Science and Technology. Springer, New York, pp 2615–2638

Niinemets Ü, Anten N (2009) Packing the photosynthetic machinery: from leaf to canopy. *In* A Laisk, L Nedbal, Govindjee, eds, Photosynthesis in Silico: Understanding Complexity from Molecules to Ecosystems. Springer, Dordrecht, The Netherlands, pp 363–399

Niinemets Ü, Tenhunen JD (1997) A model separating leaf structural and physiological effects on carbon gain along light gradients for the shade-tolerant species *Acer saccharum*. Plant Cell Environ **20:** 845–866

Ort DR, Zhu X, Melis A (2011) Optimizing antenna size to maximize photosynthetic efficiency. Plant Physiol **155:** 79–85

Parry MAJ, Andralojc PJ, Parmar S, Keys AJ, Habash D, Paul MJ, Alred R, Quick WP, Servaites JC (1997) Regulation of Rubisco by inhibitors in the light. Plant Cell Environ **20:** 528–534

Parry MAJ, Reynolds M, Salvucci ME, Raines C, Andralojc PJ, Zhu XG, Price GD, Condon AG, Furbank RT (2011) Raising yield potential of wheat. II. Increasing photosynthetic capacity and efficiency. J Exp Bot **62:** 453–467

Pask AJD, Sylvester-Bradley R, Jamieson PD, Foulkes MJ (2012) Quantifying how winter wheat crops accumulate and use nitrogen reserves during growth. Field Crops Res **126:** 104–118

Pearcy RW (1990) Sunflecks and photosynthesis in plant canopies. Annu Rev Plant Physiol Plant Mol Biol **41:** 421–453

Pearcy RW, Seemann JR (1990) Photosynthetic induction state of leaves in a soybean canopy in relation to light regulation of ribulose-1-5-bisphosphate carboxylase and stomatal conductance. Plant Physiol **94:** 628–633

Poorter H, Fiorani F, Pieruschka R, Wojciechowski T, van der Putten WH, Kleyer M, Schurr U, Postma J (2016) Pampered inside, pestered outside? Differences and similarities between plants growing in controlled conditions and in the field. New Phytol **212:** 838–855

Pound MP, French AP, Murchie EH, Pridmore TP (2014) Automated recovery of three-dimensional models of plant shoots from multiple color images. Plant Physiol **166:** 1688–1698

Powles SB, Björkman O (1981) Leaf movement in the shade species Oxalis oregana. II. Role in protection against injury by intense light. Carnegie Inst Wash Yearb **80:** 63–66

Raven JR (1994) The cost of photoinhibition to plant communities. *In* NR Baker, JR Bowyer, eds, Photoinhibition of Photosynthesis: Molecular Mechanisms to the Field. Bios Sci, Oxford, pp 449–464

Raven JA (2011) The cost of photoinhibition. Physiol Plant **142:** 87–104

Reich PB, Walters MB, Ellsworth DS, Vose JM, Volin JC, Gresham C, Bowman WD (1998) Relationships of leaf dark respiration to leaf nitrogen, specific leaf area and leaf life-span: a test across biomes and functional groups. Oecologia **114:** 471–482

Retkute R, Smith-Unna SE, Smith RW, Burgess AJ, Jensen OE, Johnson GN, Preston SP, Murchie EH (2015) Exploiting heterogeneous environments: does photosynthetic acclimation optimize carbon gain in fluctuating light? J Exp Bot **66:** 2437–2447

Reynolds M, Foulkes J, Furbank R, Griffiths S, King J, Murchie E, Parry M, Slafer G (2012) Achieving yield gains in wheat. Plant Cell Environ **35:** 1799–1823

Sassenrath-Cole GF, Pearcy RW (1994) Regulation of photosynthetic induction state by the magnitude and duration of low light exposure. Plant Physiol **105:** 1115–1123

Sharkey TD, Bernacchi CJ, Farquhar GD, Singsaas EL (2007) Fitting photosynthetic carbon dioxide response curves for C_3 leaves. Plant Cell Environ **30:** 1035–1040

Sheue CR, Liu JW, Ho JF, Yao AW, Wu YH, Das S, Tsai CC, Chu HA, Ku MS, Chesson P (2015) A variation on chloroplast development: the bizonoplast and photosynthetic efficiency in the deep-shade plant *Selaginella erythropus*. Am J Bot **102:** 500–511

Sinclair TR, Sheehy JE (1999) Erect leaves and photosynthesis in rice. Science **283:** 1455

Song Q, Zhang G, Zhu XG (2013) Optimal crop canopy architecture to maximise canopy photosynthetic CO_2 uptake under elevated CO_2: a theoretical study using a mechanistic model of canopy photosynthesis. Funct Plant Biol **40:** 109–124

Stegemann J, Timm HC, Kuppers M (1999) Simulation of photosynthetic plasticity in response to highly fluctuating light: an empirical model integrating dynamic photosynthetic induction and capacity. Trees (Berl) **14:** 145–160

Taylor SH, Long SP (2017) Slow induction of photosynthesis on shade to sun transitions in wheat may cost at least 21% of productivity. Philos Trans R Soc Lond B Biol Sci **372:** 20160543

Terashima I, Araya T, Miyazawa S, Sone K, Yano S (2005) Construction and maintenance of the optimal photosynthetic systems of the leaf, herbaceous plant and tree: an eco-developmental treatise. Ann Bot **95:** 507–519

Terashima I, Evans JR (1988) Effects of light and nitrogen nutrition on the organization of the photosynthetic apparatus in spinach. Plant Cell Physiol **29:** 143–155

Theobald JC, Mitchell RAC, Parry MAJ, Lawlor DW (1998) Estimating the excess investment in ribulose-1,5-bisphosphate carboxylase/oxygenase in leaves of spring wheat grown under elevated CO_2. Plant Physiol **118:** 945–955

Verhoeven AS, Demmig-Adams B, Adams WW III (1997) Enhanced employment of the xanthophyll cycle and thermal energy dissipation in spinach exposed to high light and N stress. Plant Physiol **113:** 817–824

Vialet-Chabrand S, Matthews JSA, Simkin AJ, Raines CA, Lawson T (2017) Importance of fluctuations in light on plant photosynthetic acclimation. Plant Physiol **173:** 2163–2179

Walters RG (2005) Towards an understanding of photosynthetic acclimation. J Exp Bot **56:** 435–447

Watling JR, Ball MC, Woodrow IE (1997) The utilization of lightflecks for growth in four Australian rain-forest species. Funct Ecol **11:** 231–239

Werner C, Ryel RJ, Correia O, Beyschlag W (2001) Effects of photoinhibition on whole-plant carbon gain assessed with a photosynthesis model. Plant Cell Environ **24:** 27–40

Weston E, Thorogood K, Vinti G, López-Juez E (2000) Light quantity controls leaf-cell and chloroplast development in Arabidopsis thaliana wild type and blue-light-perception mutants. Planta **211:** 807–815

Wu C (2011) Visual SFM: a visual structure from motion system. http://ccwu.me/vsfm (June 11, 2014)

Yamori W, Masumoto C, Fukayama H, Makino A (2012) Rubisco activase is a key regulator of non-steady-state photosynthesis at any leaf temperature and, to a lesser extent, of steady-state photosynthesis at high temperature. Plant J **71:** 871–880

Yin ZH, Johnson GN (2000) Photosynthetic acclimation of higher plants to growth in fluctuating light environments. Photosynth Res **63:** 97–107

Zadoks JC, Chang TT, Konzak CF (1974) A decimal code for the growth stages of cereals. Weed Res **14:** 415–421

Zhu XG, Long SP, Ort DR (2010) Improving photosynthetic efficiency for greater yield. Annu Rev Plant Biol **61:** 235–261

Zhu XG, Ort DR, Whitmarsh J, Long SP (2004) The slow reversibility of photosystem II thermal energy dissipation on transfer from high to low light may cause large losses in carbon gain by crop canopies: a theoretical analysis. J Exp Bot **55:** 1167–1175